

## – Supplemental Data –

### MATERIALS AND METHODS

**Materials.** Phospholipids were purchased from Avanti Polar Lipids, and 1-(4-Isothiocyanatophenyl)-3-[6,17-dihydroxy-7,10,18,21-tetraoxo-27-[N-acetylhydroxylamino) 6,11,17, 22 -tetraazaheptaecosane]thiourea (DFO-p-NCS) by Macrocyclics. The dyes 3,3'-dioctadecyloxacarbocyanine perchlorate (DiO) and Cyanine5 NHS ester were purchased from Life Technologies and Lumiprobe, respectively. ApoA-I was separated from human plasma using an established protocol (1). Antibodies for flow cytometry were purchased from eBiosciences, Biolegend, and BD Bioscience. DSPE-DFO was prepared as previously reported (2). All other reagents were acquired from Sigma-Aldrich.

**Radiochemistry.**  $^{89}\text{Zr}$  was produced at Memorial Sloan-Kettering Cancer Center on an EBCO TR19/9 variable-beam energy cyclotron (EbcO Industries Inc., British Columbia, Canada) via the  $^{89}\text{Y}(p,n)^{89}\text{Zr}$  reaction and purified in accordance with previously reported methods to yield  $^{89}\text{Zr}$  with a specific activity of 195–497 MBq/ $\mu\text{g}$  (3). Activity measurements were made using a Capintec CRC-15R Dose Calibrator (Capintec, Ramsey, NJ).

**HPLC and Radio-HPLC.** HPLC was performed on a Shimadzu HPLC system equipped with two LC-10AT pumps and an SPD-M10AVP photodiode array detector. Radio-HPLC was performed using a Lablogic Scan-RAM Radio-TLC/HPLC detector. Size exclusion chromatography was performed on a Superdex 10/300 column (GE Healthcare Life Sciences) using PBS as eluent at a flow rate of 1 mL/min.

**Transmission electron microscopy (TEM).** Different HDL nanoparticles were negatively stained with a method previously reported (4). Briefly, the original PBS-based solvent of nanoparticles was replaced with an ammonium acetate buffer. Then, the particles were mixed with a 2% sodium phosphotungstate (pH = 7.4) buffer to achieve negative stain. The mixed solution was added to TEM grids, dried, and imaged with a Hitachi H7650 system linked to a Scientific Instruments and Applications digital camera controlled by the Maxim CCD software. One-hundred-thousand-fold magnification was used to capture the images.

**Preparation of reconstituted HDL (rHDL) nanoparticles.** Reconstituted HDL was prepared by mixing 1,2-dimyristoyl-sn-glycero-3-phosphocholine (DMPC) and apoA-I in a 2.5:1 weight ratio. A lipid film was formed by evaporation of a chloroform solution containing the phospholipid. Hydration with PBS at 35 - 40 °C and sonication was followed by the addition of the required amount of apoA-I. Sonication on ice for 10 minutes yielded a slightly turbid solution that was kept at 37 °C overnight. Subsequent centrifugation at 4000 rpm for 5 min and filtration through 0.22 µm filter afforded a clear solution of rHDL. For the preparation of 1 % DSPE-DFO@rHDL, the required amount of the phospholipid-chelator DSPE-DFO (2) was added at the expense of DMPC and the same procedure was followed. Size and zeta-potential were measured on a Malvern NanoSeries Z-Sizer (Malvern, UK) in triplicate at 25 °C, allowing equilibration for 120 s and with an angle of detection of 173°.

**Modification of rHDL with desferrioxamine B.** DFO-*p*-NCS (dissolved in DMSO, 5 mg/mL) was added in steps of 5 µL to a solution of rHDL in 0.1 M PBS buffer pH 8.2, typically containing 2 mg of apoA-I per mL. The mixture was vortexed after each addition until a 2-fold molar excess of DFO-*p*-NCS over ApoA-I was achieved, and then incubated for 2 hours at 37 °C. The particles were separated from free, unreacted DFO-*p*-NCS by spin filtration using 10 kDa molecular weight cut-off (MWCO) Vivaspin 500 (Sartorius Stedim Biotech GmbH, Goettingen, Germany) tubes at 15000 rpm. The concentrate was washed 4 times with 500 µL PBS pH 7.4 and finally diluted to the final volume with PBS. The number of labels per apoA-I molecule was measured to be 1.4 ± 0.3 (n=3) by the isotope dilution method (5).

**Radiosynthesis of <sup>89</sup>Zr-apoAI-labeled rHDL, <sup>89</sup>Zr-AI-HDL.** A solution of <sup>89</sup>Zr in PBS was prepared by mixing 100 µL PBS with the corresponding volume of <sup>89</sup>Zr-oxalate solution in 1M oxalic acid and adjusted to pH 7.1 - 7.4 with 1M Na<sub>2</sub>CO<sub>3</sub>. Labeling HDL precursor DFO-apoA-I@HDL was then added as a PBS solution containing 2 mg ApoA-I/mL. The labeling mixture was prepared at an activity-to-apoA-I ratio of 1 mCi/mg ApoA-I, and incubated at 37 °C for 2 h. Subsequent isolation by spin-filtration using 10 kDa MWCO Vivaspin 500 tubes and washing with PBS (4x500 µL) afforded radiochemically pure <sup>89</sup>Zr-AI-HDL. The retentate was diluted with PBS and filtered through a 0.22 µm filter prior to use.

**Radiosynthesis of  $^{89}\text{Zr}$ -phospholipid-labeled rHDL,  $^{89}\text{Zr}$ -PL-HDL.**  $^{89}\text{Zr}$ -PL-HDL was obtained following the same procedure described above, using the corresponding labeling precursor 1 % DSPE-DFO@rHDL.

**Fluorescent HDL nanoparticles.** Fluorescently labeled DiO@rHDL was synthesized with a method similar to the one described previously (6). Briefly, phospholipids (DMPC) and DiO were mixed in chloroform solution at a weight ratio of 99:1. A thin film was formed by evaporating the solvent, and large vesicles were made by hydrating the film with apoA-1 solution. Small-sized particles were created by an ultrasonic sonication procedure and big aggregates were removed by centrifuge and filtration. Similarly, DiO@Zr-PL-HDL was prepared using the same procedure but adding 1 % DSPE-DFO at the expense of DMPC, and subsequent reaction with non-radioactive zirconium (100 ng/mg ApoA-I, as calculated from specific activity of the  $^{89}\text{Zr}$  used), added as a zirconium (IV) chloride in acetate buffer (pH 5.0). Fluorescent, non-radioactive DiO@Zr-AI-HDL was prepared by modification of DiO@rHDL with DFO as described above (Modification of rHDL with desferrioxamine B) and subsequent reaction with non-radioactive zirconium as specified above. Reaction with non-radioactive Zr was carried out at 37 °C for 2 h in PBS solution (pH 7.1-7.4), and the nanoparticles were separated from unreacted Zr by spin filtration using 10 kDa MWCO Vivaspin 500 tubes and washing with PBS (4x500  $\mu\text{L}$ ). The fluorescent HDL analogs were filtered through 0.22  $\mu\text{m}$  filters prior to use.

**Cell Culture.** The mouse breast cancer cell line 4T1 was obtained from ATCC (Manassas, VA) and grown in Dulbecco's Modified Eagle's Medium (DMEM) with 4.5 g/L L-glucose, 10% (vol/vol) heat inactivated fetal bovine serum, 100 IU penicillin, and 100  $\mu\text{g}/\text{mL}$  streptomycin and purchased from the culture media preparation facility at Memorial Sloan Kettering Cancer Center (MSKCC New York, NY).

**Animals.** Female homozygous athymic nude NCr mice were obtained from Taconic Laboratories (Hudson, NY), whereas female C57BL/6 (B6) mice were purchased from Charles Rivers Laboratories (Wilmington, MA). For orthotopic injections, mice were anesthetized with a 150 mg/kg ketamine and 15 mg/kg xylazine cocktail (10  $\mu\text{L}$ ) and an incision was made above the mammary fat pad after sterilization of the region. Then, 4T1 cells ( $1 \times 10^6$  cells in 100  $\mu\text{L}$  DMEM) were injected into the mammary fat pad, before the incision was sealed (Vetbond, 3M, St. Paul, MN) and the tumors grown for 8 days. For all intravenous injections, mice were gently warmed with a heat lamp, placed on a

restrainer, tail sterilized with alcohol pads, and the injection was placed into the lateral tail vein. All animal experiments were done in accordance with protocols approved by the Institutional Animal Care and Use Committee of MSKCC and followed National Institutes of Health guidelines for animal welfare.

**Serum Stability.** A sample of the corresponding radiolabeled HDL preparation (typically 1.5-2.0 MBq in 40-60  $\mu$ L PBS) was added to 400  $\mu$ L of FBS. The mixture was incubated at 37 °C for 24 h. Aliquots of 0.3-0.4 MBq were taken at predetermined time points (30 min, 2 h, 4 h, 8 h and 24 h) for size exclusion chromatography analysis by careful integration of the peaks.

**Blood Half-Life.** Healthy female NCr mice (8-10 weeks old, n = 6) were injected with  $1.22 \pm 0.02$  MBq (range 1.21-1.26 MBq; 30-40  $\mu$ g ApoA-I) of  $^{89}\text{Zr}$ -HDL preparation in 200  $\mu$ L PBS solution. Blood was sampled from the saphenous vein at predetermined time points (5 min, 30 min, 2 h, 8 h, 24 h and 48 h) and radioactivity measured on a Wizard<sup>2</sup> 2470 Automatic Gamma Counter (Perkin Elmer, Waltham, MA). Measurements were carried out in triplicate and the radioactivity content was calculated as the mean percentage injected dose per gram of tissue (%ID/g)  $\pm$  S.D.

**Biodistribution Studies.** Biodistribution experiments were conducted on female Black 6 mice (6-10 weeks old, n = 20) bearing orthotopic 4T1 breast tumors. The radiolabeled HDL preparation ( $1.35 \pm 0.05$  MBq, range 1.28-1.42 MBq; 35-40  $\mu$ g ApoA-I, in 200  $\mu$ L PBS solution) was administered via the lateral tail vein, and allowed to circulate for various time points (2 h, 24 h and 48 h), after which the mice were sacrificed and the organs perfused. The radioactive content in tissues of interest (blood, tumor, large and small intestines, stomach, kidneys, brain, bone, liver, lungs, heart, skin, spleen, bladder, tail) was measured using a 2470 Wizard<sup>2</sup> Automatic Gamma Counter (Perkin Elmer, Waltham, MA) and the tissue associated activity was calculated as the mean percentage injected dose per gram of tissue (%ID/g)  $\pm$  S.D.

**autoradiography.** Following sacrifice, liver, spleen, tumor and muscle tissues were excised and embedded in OCT mounting medium (Sakura Finetek, Torrance, CA), frozen on dry ice, and a series of 10  $\mu$ m thick frozen sections cut. To determine radiotracer distribution, digital autoradiography was performed by placing tissue sections in a film cassette against a phosphor imaging plate (BASMS-2325, Fujifilm, Valhalla, NY) for 48 h at -20 °C. Phosphor imaging plates were read at a pixel resolution of 25  $\mu$ m with a Typhoon 7000IP plate reader (GE Healthcare, Pittsburgh, PA). After autoradiographic

exposure, the same frozen sections were then used for immunohistochemical staining and imaging.

**Staining/Microscopy.** Tissue sections (10  $\mu\text{m}$  thickness, frozen) were stained for CD31 with anti-CD31 antibodies (Dianova, Hamburg, Germany) followed by a biotinylated goat anti-rat secondary antibody (Vector Labs, Burlingame, CA), streptavidin-HRP D (Ventana Medical Systems, Tucson, AZ) and finally tyramide Alexa Fluor 488 (Invitrogen, Carlsbad, CA). The same sections were stained for Iba1 with anti-Iba1 rabbit polyclonal antibody (Wako, Richmond, VA) followed by a biotinylated goat anti-rabbit secondary antibody (VECTASTAIN<sup>®</sup> ABC kit, Vector Labs, Burlingame, CA), streptavidin-HRP D, and tyramide Alexa Fluor 568 (Invitrogen, Carlsbad, CA) for fluorescent signal (VECTASTAIN<sup>®</sup> ABC kit, Vector Labs, Burlingame, CA). Additional nuclear staining was performed using 4',6-Diamidino-2-phenylindole dihydrochloride (DAPI, Sigma Aldrich, St. Louis, MO). All sections were counterstained with hematoxylin & eosin (H&E) solution. All images were obtained using an EVOS FL Auto digital inverted fluorescence microscope (Life Technologies, Norwalk, CT). Fluorescent images were obtained at 4 $\times$  magnification, while brightfield images were obtained at both the 4 $\times$  and 20 $\times$  magnification. On stained sections, Iba1 fluorescence was observed using a Texas Red light cube (Ex 585/29, Em 624/40, EVOS LED Light cube), while CD31 fluorescence was observed using a GFP light cube (Ex 470/22, Em 510/42, EVOS LED Light cube).

**PET/CT Imaging.** Female C57BL/6 (B6) mice (8-10 weeks old,  $n = 8$ ) bearing 4T1 breast tumors were injected with  $7.1 \pm 0.2$  MBq (range 6.7-7.2 MBq) <sup>89</sup>Zr-HDL (180-200  $\mu\text{g}$  apoA-I) in 200  $\mu\text{L}$  PBS solution via the lateral tail vein. At 24h the animals were anesthetized with isofluorane (Baxter Healthcare, Deerfield, IL)/oxygen gas mixture (2% for induction, 1 % for maintenance) and a scan was then performed using an Inveon PET/CT scanner (Siemens Healthcare Global, Erlangen, Germany). Whole body PET static scans recording a minimum of 50 million coincident events were performed, with a duration of 15 min. The energy and coincidence timing windows were 350–700 keV and 6 ns, respectively. The image data were normalized to correct for non-uniformity of response of the PET, dead-time count losses, positron branching ratio, and physical decay to the time of injection, but no attenuation, scatter, or partial-volume averaging correction was applied. The counting rates in the reconstructed images were converted to activity concentrations (percentage injected dose [%ID] per gram of tissue) by use of a

system calibration factor derived from the imaging of a mouse-sized water-equivalent phantom containing  $^{89}\text{Zr}$ . Images were analyzed using ASIPro VMTM software (Concorde Microsystems, Knoxville, TN). Quantification of activity concentration was done by averaging the maximum values in at least 5 ROIs drawn on adjacent slices of the tissue of interest (7). Whole body standard low magnification CT scans were performed with the X-ray tube setup at a voltage of 80 kV and current of 500  $\mu\text{A}$ . The CT scan was acquired using 120 rotational steps for a total of 220 degrees yielding an estimated scan time of 120 s with an exposure of 145 ms per frame.

**Flow cytometry.** Murine 4T1 breast cancer tumors were orthotopically implanted as described above in female C57BL/6 (B6) mice. On day 8 after implantation, animals were injected with the corresponding fluorescent rHDL analogs at 0.1 mg DiO/kg body weight. The nanoparticles were allowed to circulate for 24 h and then tumors were excised, diced, and digested with a cocktail of enzymes, including liberase TH (Roche), hyaluronidase (Sigma-Aldrich), and DNase (Sigma-Aldrich), in a 37 °C oven for one hour. Single-cell suspension was made by removing tissue aggregates, extracellular matrix, and cell debris from the solution. The same flow cytometry setting was applied to all samples. DiO was detected on the FITC channel. All samples were measured on an LSRFortessa (BD Biosciences, San Jose, CA) flow cytometer. Results were analyzed with FlowJo (Ashland, OR) and statistics were calculated with Prism (GraphPad, La Jolla, CA). The antibodies and clones used are listed in the table below and the gating procedure is shown in figure S2.

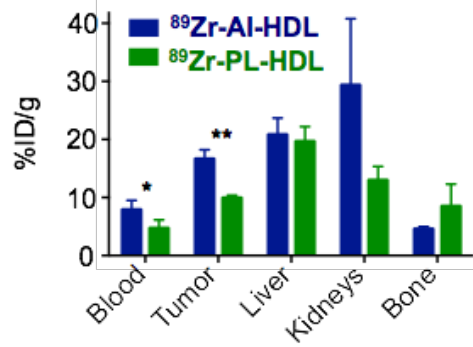
<b>Antibody</b>	<b>Clone</b>	<b>Source</b>
Ly6C	HK1.4	eBioscience
MHCII (I-A/I-E)	M5/114.152	eBioscience
CD45	30-F11	Biolegend
CD64	X54-5/7.1	Biolegend
CD11b	M1/70	eBioscience
CD3	17A2	Biolegend
CD31	13.3	BD Biosciences
CD11c	M418	eBioscience

**Supplemental Table 1.** Tissue radioactivity distribution of  $^{89}\text{Zr}$ -AI-HDL in female C57BL/6 (B6) mice bearing orthotopic 4T1 breast cancer tumors. Data presented as mean %ID/g  $\pm$  SD (n  $\geq$  3 for each time point).

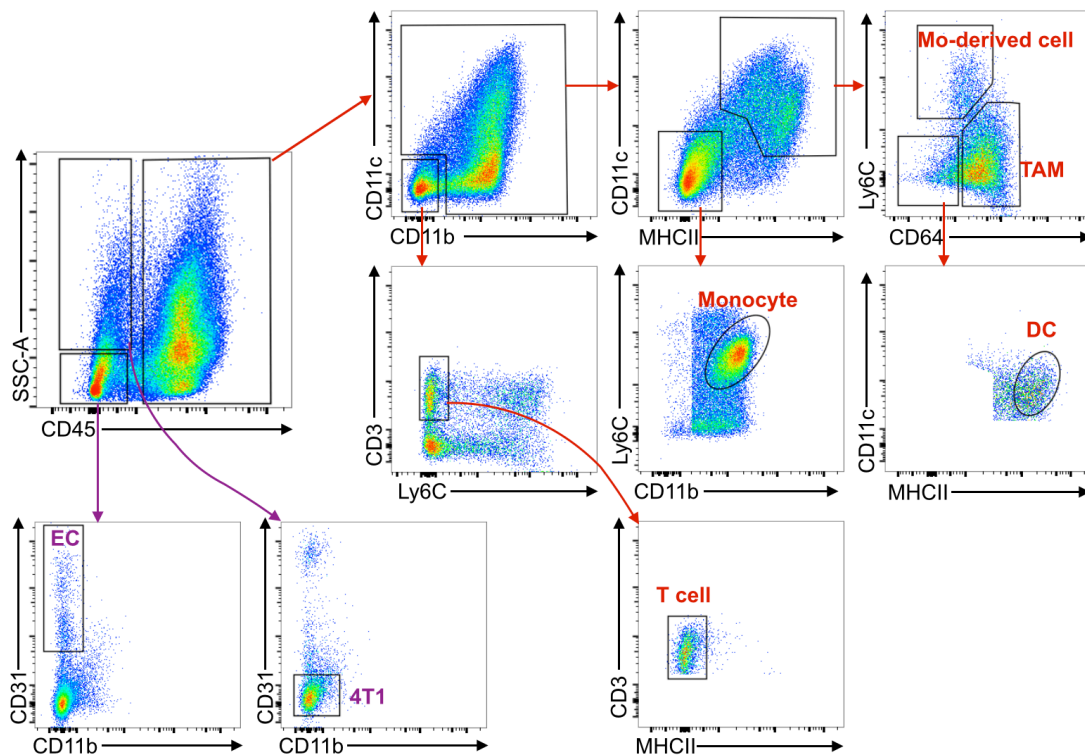
Tissue	2 h	24 h	48 h
Blood	34.5 $\pm$ 6.9	5.30 $\pm$ 0.94	0.98 $\pm$ 0.25
Tumor	4.53 $\pm$ 0.76	16.5 $\pm$ 2.8	12.3 $\pm$ 4.5
Heart	2.67 $\pm$ 0.81	3.05 $\pm$ 0.17	2.23 $\pm$ 0.57
Lungs	1.34 $\pm$ 0.60	2.14 $\pm$ 0.65	1.63 $\pm$ 0.53
Liver	7.51 $\pm$ 2.21	14.6 $\pm$ 0.54	12.8 $\pm$ 4.5
Gall Bladder	5.47 $\pm$ 1.85	5.18 $\pm$ 2.75	2.86 $\pm$ 1.83
Spleen	5.02 $\pm$ 1.20	8.44 $\pm$ 0.27	5.65 $\pm$ 1.73
Pancreas	2.23 $\pm$ 1.96	1.39 $\pm$ 0.38	1.03 $\pm$ 0.32
Stomach	1.68 $\pm$ 0.35	1.97 $\pm$ 0.07	1.54 $\pm$ 0.17
Small Intestine	2.22 $\pm$ 0.53	2.67 $\pm$ 0.37	1.72 $\pm$ 0.38
Large Intestine	1.90 $\pm$ 0.39	4.71 $\pm$ 0.10	3.87 $\pm$ 0.67
Kidney	16.4 $\pm$ 2.1	21.2 $\pm$ 1.87	18.1 $\pm$ 4.3
Muscle	1.27 $\pm$ 0.45	1.23 $\pm$ 0.36	0.75 $\pm$ 0.27
Bone	3.60 $\pm$ 0.71	3.32 $\pm$ 0.04	2.70 $\pm$ 0.62
Skin	1.90 $\pm$ 0.91	2.18 $\pm$ 0.09	3.91 $\pm$ 2.11

**Supplemental Table 2.** Tissue radioactivity distribution of  $^{89}\text{Zr}$ -PL-HDL in female C57BL/6 (B6) mice bearing orthotopic 4T1 breast cancer tumors. Data presented as mean %ID/g  $\pm$  SD (n  $\geq$  3 for each time point).

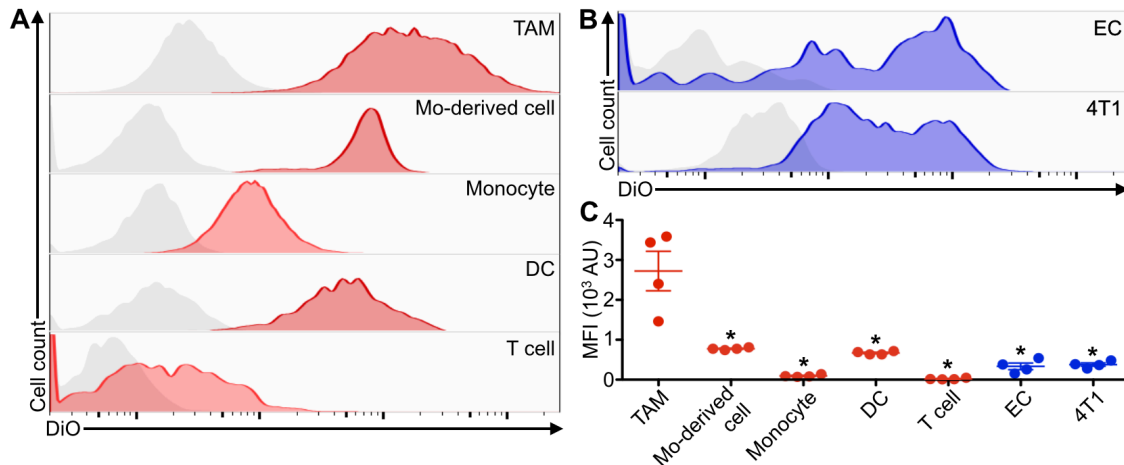
Tissue	2 h	24 h	48 h
Blood	23.7 $\pm$ 1.51	2.19 $\pm$ 0.23	0.49 $\pm$ 0.06
Tumor	3.78 $\pm$ 0.50	8.55 $\pm$ 1.30	12.0 $\pm$ 4.7
Heart	1.68 $\pm$ 0.10	1.26 $\pm$ 0.16	1.61 $\pm$ 0.25
Lungs	1.58 $\pm$ 0.72	1.34 $\pm$ 0.46	1.43 $\pm$ 0.50
Liver	14.1 $\pm$ 1.50	13.6 $\pm$ 2.5	15.2 $\pm$ 2.5
Gall Bladder	43.5 $\pm$ 19.9	2.27 $\pm$ 0.91	0.69 $\pm$ 0.20
Spleen	7.24 $\pm$ 0.44	5.37 $\pm$ 1.23	6.48 $\pm$ 1.97
Pancreas	1.25 $\pm$ 0.67	0.90 $\pm$ 0.27	0.80 $\pm$ 0.24
Stomach	1.47 $\pm$ 0.31	1.32 $\pm$ 0.02	1.14 $\pm$ 0.18
Small Intestine	2.93 $\pm$ 0.40	1.52 $\pm$ 0.06	1.77 $\pm$ 0.68
Large Intestine	1.16 $\pm$ 0.17	1.45 $\pm$ 0.04	1.28 $\pm$ 0.21
Kidney	13.1 $\pm$ 1.7	13.2 $\pm$ 3.6	13.3 $\pm$ 2.3
Muscle	0.99 $\pm$ 0.18	1.03 $\pm$ 0.42	0.73 $\pm$ 0.30
Bone	5.80 $\pm$ 1.43	15.5 $\pm$ 1.9	17.1 $\pm$ 4.8
Skin	1.90 $\pm$ 0.45	1.76 $\pm$ 0.22	2.04 $\pm$ 0.99



**Supplemental Figure 1. PET-quantified radioactivity accumulation in selected tissues.** Data are presented as mean %ID/g  $\pm$  SD (n = 4 for both nanotracers) measured from PET images collected at 24 h post injection. \*  $P < 0.05$ , \*\*  $P < 0.01$ .



**Supplemental Figure 2. Gating procedure to identify cells in tumor.** Live single cells were subjected to the above gating procedure to identify tumor-associated macrophages (TAM), monocyte-derived cells (Mo-derived cell), monocytes, dendritic cells (DC), T cells, endothelial cells (EC), and tumor cells (4T1).



**Supplemental Figure 3. Plain, Zr-free rHDL targets tumor-associated macrophages.**

4T1-cell-induced orthotopic breast tumors were used to isolate single cells. A) Representative DiO levels in five immune cells, namely tumor-associated macrophages (TAM), monocyte-derived cells (Mo-derived cell), monocytes, dendritic cells (DC), and T cells. B) Representative DiO levels in endothelial cells (EC) and tumor cells (4T1). Cells from a PBS-injected mouse serve as controls (grey histograms to the left). C) Quantification of DiO levels presented as mean fluorescence intensity (MFI). Statistics was calculated with two-tailed Student's *t*-test with unequal variance by comparing to TAM. \*  $P < 0.05$ .

## References

1. McPherson PAC, Young IS, McKibben B, McEneny J. High density lipoprotein subfractions: isolation, composition, and their duplicitous role in oxidation. *J Lipid Res.* 2007;48:86-95.
2. Perez-Medina C, Abdel-Atti D, Zhang Y, Longo VA, Irwin CP, Binderup T, Ruiz-Cabello J et al. A modular labeling strategy for in vivo PET and near-infrared fluorescence imaging of nanoparticle tumor targeting. *J Nucl Med.* 2014;55:1706-1711.
3. Holland JP, Sheh Y, Lewis JS. Standardized methods for the production of high specific-activity zirconium-89. *Nucl Med Biol.* 2009;36:729-739.
4. Forte TM, Nordhausen RW. Electron microscopy of negatively stained lipoproteins. *Methods Enzymol.* 1986;128:442-457.
5. Perk LR, Vosjan MJ, Visser GW, Budde M, Jurek P, Kiefer GE, van Dongen GA. p-Isothiocyanatobenzyl-desferrioxamine: a new bifunctional chelate for facile radiolabeling of monoclonal antibodies with zirconium-89 for immuno-PET imaging. *Eur J Nucl Med Mol Imaging.* 2010;37:250-259.
6. Duivenvoorden R, Tang J, Cormode DP, Mieszawska AJ, Izquierdo-Garcia D, Ozcan C, Otten MJ et al. A statin-loaded reconstituted high-density lipoprotein nanoparticle inhibits atherosclerotic plaque inflammation. *Nat Commun.* 2014;5:3065.
7. Smith-Jones PM, Solit DB. Generation of DOTA-conjugated antibody fragments for radioimmunoimaging. *Methods Enzymol.* 2004;386:262-275.